Reverse Osmosis of Nonaqueous Solutions through Porous Silica-Zirconia Membranes

Toshinori Tsuru, Masashi Miyawaki, Tomohisa Yoshioka, and Masashi Asaeda
Dept. of Chemical Engineering, Hiroshima University, Higashi-Hiroshima, 739-8527, Japan

DOI 10.1002/aic.10654
Published online September 28, 2005 in Wiley InterScience (www.interscience.wiley.com).

Porous silica-zirconia membranes with pore diameters from 0.8 to 2 nm were prepared by a sol-gel process, and applied to the separation of alcohols (hexanol, octanol, decanol) and alkanes (hexane, decane, tetradecane) in ethanol solutions by reverse osmosis over the temperature range from 25 to 60° C. A silica-zirconia membrane with a pore diameter of 1 nm showed a molecular weight-cut-off (MWCO) of 200 in ethanol solutions. Rejection increased with the applied pressure, for both alcohol and alkane solutes. However, the rejection of alcohols was found to decrease with temperature, while that for alkanes remained nearly constant. The separation characteristics were examined for the following membrane parameters: solvent permeability, L_p*, reflection coefficient,* σ*, and solute permeability,* P*, based on the Spiegler-Kedem equation. The viscosity of solutions and the diffusivity of alkanes and alcohol solutes in nano-sized pores were found to show a larger temperature dependency than in bulk. The diffusivity of alkane solutes showed the same temperature dependency as the viscosity of ethanol in nano-sized pores, while the diffusivity of alcohol solutes showed a larger temperature dependency than the viscosity of ethanol, probably because of a larger interaction between alcohol solutes and the hydrophilic surface of silica-zirconia membranes. Diffusion experiments were carried out to confirm the temperature dependency of the diffusivities in nano-sized pores. A bilayer model verified that solute permeabilities by reverse osmosis and diffusion experiments were consistent with each other.* © 2005 American Institute of Chemical Engineers *AIChE J,* 52: 522–531, 2006

Keywords: reverse osmosis, nanofiltration, inorganic membranes, silica-zirconia, diffusion, rejection, nonaqueous solutions

Introduction

Reverse osmosis and nanofiltration membranes have been developed for applications that involve the processing of aqueous solutions, such as the purification of drinking water and wastewater treatment. One of the potential applications is separation in nonaqueous solutions, including the separation of mixed solvents and the concentration of macromolecules in organic solvents. Extensive investigations in pressure-driven membrane separation, such as reverse osmosis and nanofiltration, have been reported in attempts to utilize polymeric membranes for nonaqueous solutions.[1-4] Whu et al.[2] reported on the nanofiltration of methanol solutions using solvent resistant-polymeric membranes. Bhanushali et al.[3] investigated the use of nanofiltration rejection in the rejection of organic dyes and triglycerides in polar (methanol, ethanol) and nonpolar (hexane) solvents. The interaction among membrane materials, solvents, and solutes were emphasized. Peeva et al.[4] reported on permeate volumetric fluxes and the rejection of docosane and tetraoctylammonium as a model solute in toluene solutions, and successfully analyzed the performance of the membranes based on the solution-diffusion model combined with concentration polarization, which are typically applied to aqueous systems. However, the instability of membranes in non-

Correspondence concerning this article should be addressed to T. Tsuru at tsuru@hiroshima-u.ac.jp.

aqueous solutions represents a major drawback to the use of polymeric membranes, although solvent-resistant polymeric membranes have been reported.[5]

Inorganic membranes, which have an inherently excellent resistance to a wide variety of solvents, have attracted a great deal of interest.[6-9] At present, the available experimental data on reverse osmosis and nanofiltration performance is very limited since inorganic porous membranes having pore diameters less than several nm have been developed only recently. Buekenhoudt et al.[10] compared the performance between ceramic and solvent-resistant-polymeric membranes, and found that ceramic membranes could be successfully used in the separation of pharmaceutical components in methylene chloride as well as the recovery of homogeneous catalysts in isopropanol. We also reported on the application of inorganic porous membranes to the permeation of pure solvents[9,11] and the nanofiltration of polyethylene glycols in alcohol solutions.[12,13] A wide variety of solvents and solutes can be separated in pressure-driven membrane separation systems, such as reverse osmosis, nanofiltration, ultrafiltration, and microfiltration. In the present study, our focus was on the separation of low molecular weight organic solvents (less than 200) in ethanol, which can be categorized into the reverse osmosis range.

From the viewpoint of the transport mechanism through porous membranes, the solution-diffusion model and the non-equilibrium model have been successfully applied to a wide variety of aqueous systems. The solution-diffusion model, which considers the contribution of diffusion to solute transport and neglects the contribution of convection, has been widely applied to nonporous membranes, such as polymeric reverse osmosis membranes.[14] On the other hand, non-equilibrium thermodynamic models, such as the Spiegler-Kedem model,[15] can be applied, in principle, to any type of membrane system, including nonporous and porous membranes. Bhanushali et al.[3] evaluated the permeation characteristics in nonaqueous solutions based on the solution-diffusion model and the Spiegler-Kedem model, and concluded that the solution-diffusion model is not applicable because of the coupling between solute and solvent fluxes. However, at present no universally accepted model for nonaqueous solutions is available, and the non-equilibrium thermodynamic model needs to be examined for its possible application.

It is also noteworthy that the advantage of using membranes to discuss the transport mechanism through porous materials, which has been extensively investigated using powdered porous materials, might be a useful approach. Restricted diffusion of a variety of solutes and solvents through porous materials is an important issue, not only in membrane separation but also in catalysts, adsorption, and related processes, and has been investigated in terms of temperature and concentration dependency.[16] The diffusivity has been determined based on measurements of concentration change as a function of time and curve-fitting with mathematical diffusion models,[17] while steady-state data can be used to obtain diffusivity in the case of membrane separation. Another advantage would be the possibility to evaluate the effect of viscosity on the diffusivity in nano-sized pores. Diffusivity is affected by the viscosity of solutions, as is well understood from correlation equations such as the Wilke-Chang equation, where diffusivity is formulated using the inverse of viscosity.[18] However, the dependency of diffusivity on viscosity in pores, especially nano-sized pores, which may not be the same as in bulk solutions, is difficult to measure for the case of powered materials. On the other hand, in the case of membrane separation, the effect of viscosity can be evaluated based on the measurements of permeability measurement, as will be discussed below in the Theory section.

In the present study, silica-zirconia porous membranes having approximate pore diameters of 0.8 to 2 nm were fabricated by a sol-gel process, and were employed for the reverse osmosis of nonaqueous solutions containing organic solutes, such as alcohols and alkanes in ethanol solutions, at different applied pressures and temperatures. Membrane parameters: solute permeability, reflection coefficient, and solvent permeability, which were obtained using the Spiegler-Kedem equation, were investigated in terms of temperature dependency. Moreover, diffusion experiments were carried out and the results were compared with those obtained by reverse osmosis.

Theory

Reverse osmosis based on non-equilibrium thermodynamics

Pressure-driven separation performance, including reverse osmosis as well as ultrafiltration, has been successfully analyzed based on the non-equilibrium thermodynamic model.[19-21] Volume flux (J_v) and solute flux (J_s) through a membrane, which was originally derived by Kedem-Katchalsky, based on non-equilibrium thermodynamics, was formulated for reverse osmosis by Spiegler and Kedem,[15] as follows:

$$J_v = L_p(\Delta P - \sigma\Delta\pi) \tag{1}$$

$$J_s = -D_{eff}\frac{d}{dx}C + (1-\sigma)CJ_v \tag{2}$$

where L_p and σ represent the solvent permeability and reflection coefficient, respectively; ΔP and $\Delta\pi$ are the differences in applied pressure and osmotic pressure, respectively. Eq. 1 indicates that J_v is the product of pure solvent permeability, L_p, and the effective transmembrane pressure, $\Delta P - \sigma\Delta\pi$. If the mechanism of transport through porous membranes obeys the viscous flow mechanism, the volumetric permeability, L_p, can be interpreted with the following equation, based on the Hagen-Poiseuille flow:

$$L_p = \frac{\pi r_p^4}{8\Delta x}\frac{N}{\mu} \tag{3}$$

where r_p is the effective pore radius, Δx the effective thickness of a membrane, N the number of pores, and μ the viscosity of solution in the pores.

In Eq. 2, the first and second term show the contribution of diffusion and convection, respectively, to solute flux. The effective diffusivity, D_{eff}, through membrane pores having separation ability is reported to be different from diffusivity in a bulk solution, D_{bulk}, because of restricted diffusion. Solute transport by convection is also restricted, and σ can be interpreted as the fraction of solute transported by convective flow. By integrating Eq. 2 from the feed to the permeate stream (membrane thickness, Δx), with the aid of the reverse osmosis

condition ($J_s = C_p J_v$), rejection, which is defined as $R = 1 - C_p/C_f$, can be expressed with the following equations:

$$R = \frac{(1 - F)\sigma}{1 - \sigma F} \tag{4}$$

where

$$P = D_{eff}/\Delta x \tag{5}$$

$$F = exp\left(- \frac{(1 - \sigma)J_v}{P} \right) \tag{6}$$

σ, P, and L_p are referred to membrane parameters, which determine the separation performances in reverse osmosis and ultrafiltration.[19,21] It should be noted that the transport equations derived by Deen[20] are expressed in a manner similar to the Spiegler-Kedem equation.

Diffusivity measurement

Diffusivity though a porous membrane (membrane area: A) can be determined based on the results of diffusion experiments using two compartment cells, where a solute at a concentration of C_1 in a feed-side compartment (volume: V_1) diffuses to the permeate-side compartment (concentration of C_2, volume V_2). Transport in a dilute concentration can be expressed with the following quasi-steady-state diffusion in a membrane and the material balance in cell 2, using permeability, P_D, determined by diffusion experiment.

$$J_s = P_D(C_1 - C_2) = \frac{V_2}{A}\frac{dC_2}{dt} \tag{7}$$

With the aid of the following boundary conditions,

$$t = 0 : C_1 = C_1^0,\ C_2 = 0 \tag{8}$$

$$t = \infty : C_1 = C_2 = C^\infty = (C_1^0 V_1 + C_2^0 V_2)/(V_1 + V_2) \tag{9}$$

integration of Eq. 7 gives the concentration of the permeate stream, C_2, as a function of t as follows:

$$ln\left\{ 1 - \frac{C_2}{C^\infty} \right\} = - \frac{(V_1 + V_2)}{V_1 \cdot V_2} A P_D t \cong - \frac{1}{V_2} A P_D t \tag{10}$$

If $V_1 \gg V_2$, then Eq. 10 can be simplified to the last expressions.

Experimental Procedures

Preparation of silica-zirconia membranes

Silica-Zirconia colloidal sols, the molar ratio of Si/Zr of which was adjusted to 0.9/0.1, were prepared by hydrolysis and the condensation of tetraethoxysilane (TEOS) and zirconium tetra-*n*-butoxide using an acid catalyst (HCl). The colloidal sols were coated on the outer surface of substrates (cylindrical α-alumina microfiltration membranes with an average pore diameter of 1 μm; outer and inner diameter of 10 and 8 mm, respectively; a length of 9 cm; porosity 0.5), and fired at 500°C. Both ends of the substrates were connected to glass tubes; one end of which was sealed, while the other end was used for the permeate stream. The average pore sizes of silica-zirconia membranes were controlled by the appropriate choice of colloidal diameters used for the coating. The procedure for the preparation of porous membranes has been described in detail in our previous article.[12,22]

The pore size distribution of the porous membranes was estimated by nanopermporometry.[23] In the case of nanopermporometry where a mixture of a noncondensable gas, such as N_2, and a condensable gas (vapor), such as H_2O, is fed to the porous membranes and the permeability of the non-condensable gas is measured, the vapor is assumed to be capillary-condensed in membrane pores that are smaller than the following Kelvin diameter, d_K, thus blocking the permeation of the non-condensable gas.

$$d_K = -4v\sigma \cos\theta/(RT \ln(P/P_s)) \tag{11}$$

with θ: contact angle, σ: surface tension, v: molar volume, P: vapor pressure, and P_s: saturation vapor pressure. The Kelvin diameters increase with the vapor pressure of a condensable gas in the feed. By measuring the permeability of the non-condensable gas as a function of relative pressure, P/P_s, it is possible to estimate the pore size distribution. Details of the experimental apparatus have been described in our previous article.[22,23] Several types of membranes having different average pore sizes in a range of 0.8 to 2.5 nm, as determined by nanopermporometry, were used in the present study.

Reverse osmosis experiments

The solutes used were alkanes (hexane (molecular weight 86), cyclohexane (84), decane (142), tetradecane (198)), alcohols (hexanol (102), octanol (130), decanol (158)), and hexanediol (118) and dissolved in ethanol as a model nonaqueous system. The reverse osmosis of each solute in ethanol solutions was carried out using the experimental apparatus shown in Figure 1 under a total recycle system where the retentate and the permeate were recycled to the feed tank, thus maintaining the feed concentration constant at 1 mol %. A silica-zirconia membrane was installed vertically inside a reverse osmosis cell with an inner diameter of 4 cm. The feed solution, pressurized with a plunger pump in the range of 0.5-3.0 MPa, was vigorously agitated using a magnetic stirrer at 600 rpm to minimize the effect of concentration polarization. The reverse osmosis experiments were carried out from higher to lower pressure after confirming the steady state (constant flux and permeate concentration). The retentate stream was recycled at an approximate flow rate of 20 mL/min to the feed tank. The permeate stream was maintained at atmospheric pressure, and collected using a sample tube immersed in an ice bath. The temperature of the feed solution was controlled at 25-60°C using a tape heater. Pure ethanol was permeated for more than one day after the reverse osmosis experiment of each solute. Solute concentrations were determined by a gas chromatograph equipped with a packed column of Gaschropack 54 at an operating temperature of 180°C and a thermal conductivity detector (TCD). The ethanol and other chemicals were purchased from

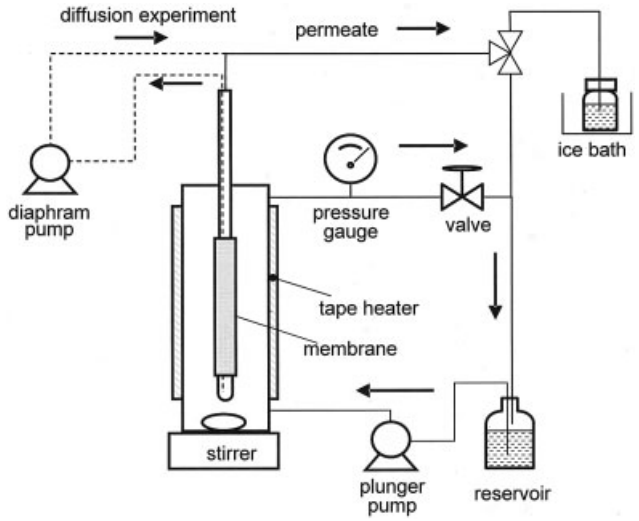

Figure 1. Experimental apparatus used for the reverse osmosis of nonaqueous solutions.

(Diffusion experiments were carried out using a permeate stream shown with broken lines.)

Katayama Chemical (Osaka, Japan) and were used without further purification.

Diffusion experiments

Diffusion experiments involving ethanol solutions of hexane and decane were carried out using the same apparatus as was used for the reverse osmosis. The volume of the feed side stream, including the volume of the reservoir, was 1500 mL, while that of the permeate stream was approximately 20 mL, which was precisely determined by collecting all liquid in the permeate stream using a diaphragm pump. The permeate stream was recycled from the bottom of the inside of a tubular membrane using a diaphragm pump at an approximate flow rate of 5 mL/min, which permits complete mixing in the permeate stream, while the feed stream was agitated by means of a magnetic stirrer. The initial concentration of the feed-side stream was 1 mol %, while that of the permeate stream was zero. Since the feed side volume was sufficiently large, no change in the feed side concentration was detected.

Results and Discussion

Reverse osmosis performance in ethanol solutions

Figure 2 shows the pore size distributions where the dimensionless permeability of nitrogen (DPN), normalized with the permeability of pure nitrogen, is plotted as a function of Kelvin diameters. The DPN decreased with increasing Kelvin diameter, which corresponds to an increase in the vapor pressure of H_2O in the feed, because the permeation of nitrogen was blocked by the capillary-condensed H_2O. The DPN finally reached zero for the three membranes; no permeation of nitrogen was detected through pores with a Kelvin diameter larger than several nm, suggesting that no pinholes larger than several nm were present. The average pore sizes, determined at 50% DPN, were 0.8, 1.0, and 1.7 nm, for membranes M-0.8, M-1.0, and M-1.7, respectively. Figure 3 shows the permeate weight-based flux, J_w, and rejection, R, as a function of molecular

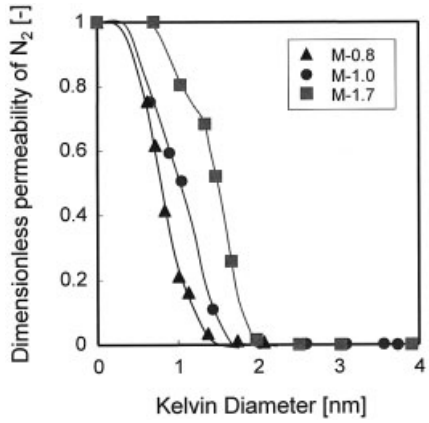

Figure 2. Dimensionless permeability of nitrogen as a function of Kelvin diameter for three silica-zirconia membranes with average pore sizes of 0.8, 1.0, and 1.7 nm.

(H_2O vapor was used for capillary-condensed vapor.)

weights of the alkane and alcohol solutes in ethanol for M-0.8, M-1.0, and M-1.7. It is evident that the permeate flux increased with an increase in pore size, while the rejection of solutes increased with a decrease in pore size. The molecular weight-

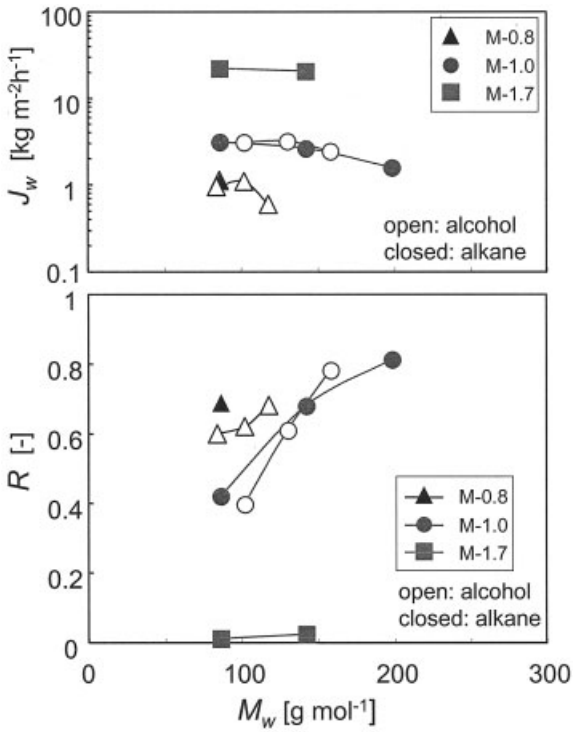

Figure 3. Permeate volume flux and rejection as a function of the molecular weights of alkane and alcohol solutes in ethanol solutions for M-0.8, M-1.0, and M-1.7 (permeation temperature: 60° C; applied pressure: 3 MPa (M-0.8, M-1.0) and 2 MPa (M-1.7); solutes: hexane (MW 86.2), decane (142.3), tetradecane (198.4), hexanol (102), octanol (130.2), decanol (158.3)).

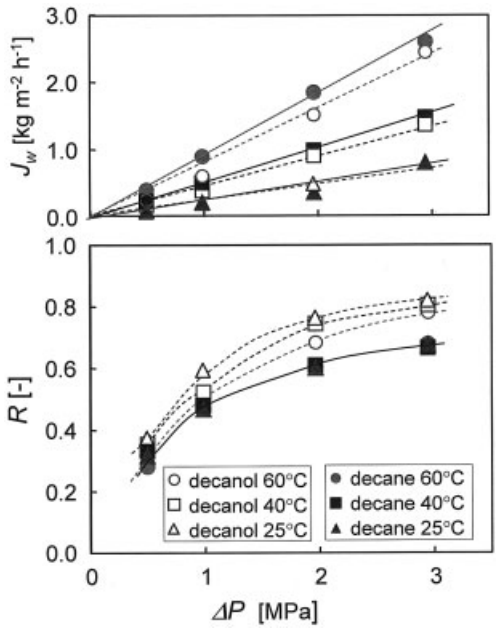

Figure 4. Permeate volume flux and rejection as a function of applied pressure for decane (black symbols) and decanol (white symbols) in ethanol solutions (M1.0; permeation temperature: 25, 40, and 60° C).

cut-off (MWCO), determined at 90% of rejection, for M-1.0 can be estimated to be several hundreds, while M-1.7 showed approximately no rejection for the solutes used. Therefore, it can be concluded that pore sizes smaller than 1.5 nm would be required for the separation of organic molecules with molecular weights of several hundreds in ethanol solutions. Considering the molecular size, based on the Lennard-Jones potential parameter, of ethanol is reported as 0.45 nm and that of hexane 0.59 nm,[18] it was suggested that the rejection of solutes occurred mainly based on the molecular sieving effect. J_w appears to decrease with the molecular weight of the solute; however, the decreased flux was found to recover with time by permeating pure ethanol to approximately the same level as the initial flux of ethanol. Since the solutes used for the separation experiments appeared to plug the membrane pores, pure ethanol was permeated for more than one day to remove any plugged solute.

Figure 4 shows values for the permeate weight flux, J_w, and rejection, R, for decanol and decane in ethanol solutions using membrane M-1.0 as a function of applied pressure. The permeate flux, J_w, increased proportionately with applied pressure, the driving force for the separation by reverse osmosis, and increased with temperature because of the lower viscosity. Decanol appears to show a lower J_w than decane. This can be explained as follows. Most inorganic materials have a hydrophilic tendency because their surfaces are hydrolyzed to form hydroxyl groups, such as silanol groups (-SiOH). Therefore, decanol would adsorb more strongly to membrane pores than decane, and consequently block the permeation of solutions. In terms of rejection of solutes, both solutes show an increased rejection with an increase in applied pressure, which is a typical tendency of reverse osmosis membranes.[21] On the other hand, the rejection of decanol decreased with temperature, showing a consistent tendency observed for aqueous solutions,[21] while that of decane was nearly constant. Figures 5a and b show the rejection for alkanes and alcohols at an applied pressure of 3.0 MPa as a function of temperature for M-1.0 and M-0.8 (average pore size: 0.8 nm), respectively. The rejection of alkanes (tetradecane, decane, hexane) was nearly constant, irrespective of temperature, while that for alcohols (decanol, octanol, hexanol) and hexanediol decreased with temperature. The rejection dependency on temperature was confirmed using two different membranes, M-1.0 and M-0.8. The interaction between solutes and the membrane obviously plays an important role in determining the temperature dependency of rejection, and will be further discussed below.

Membrane parameters based on the transport model

As shown in Figure 4, rejection is dependent upon applied pressure, and this tendency can be analyzed based on the Spiegler-Kedem equations.[12] Figure 6a shows the rejection of decane and decanol as a function of the inverse of the permeate volumetric flux, J_v, obtained after converting from weight-based flux, J_w, at the permeation temperatures, while Figure 6b

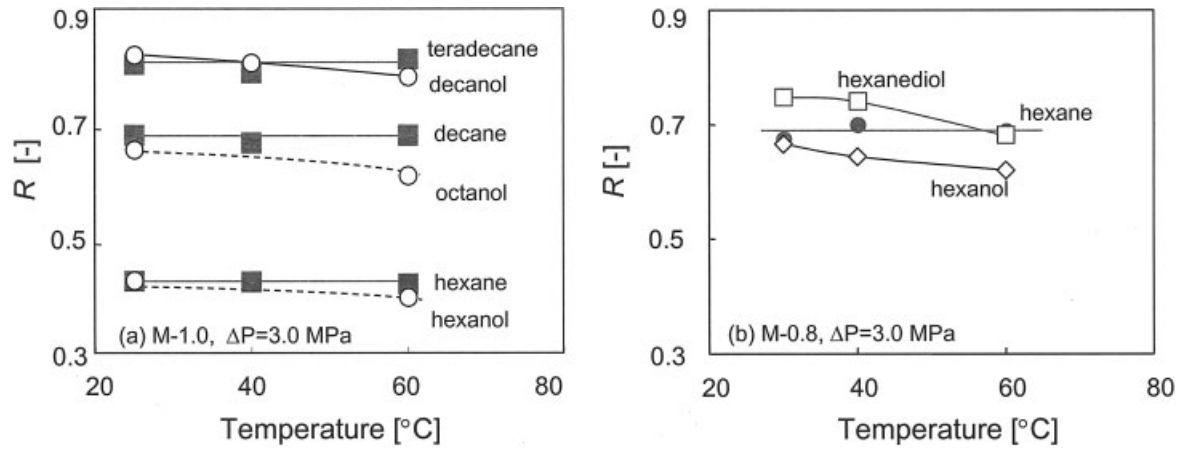

Figure 5. Temperature dependency of rejections of alcohols (white symbols) and alkanes (black symbols) using M-1.0 (a) and M-0.8 (b) (applied pressure: 3.0 MPa).

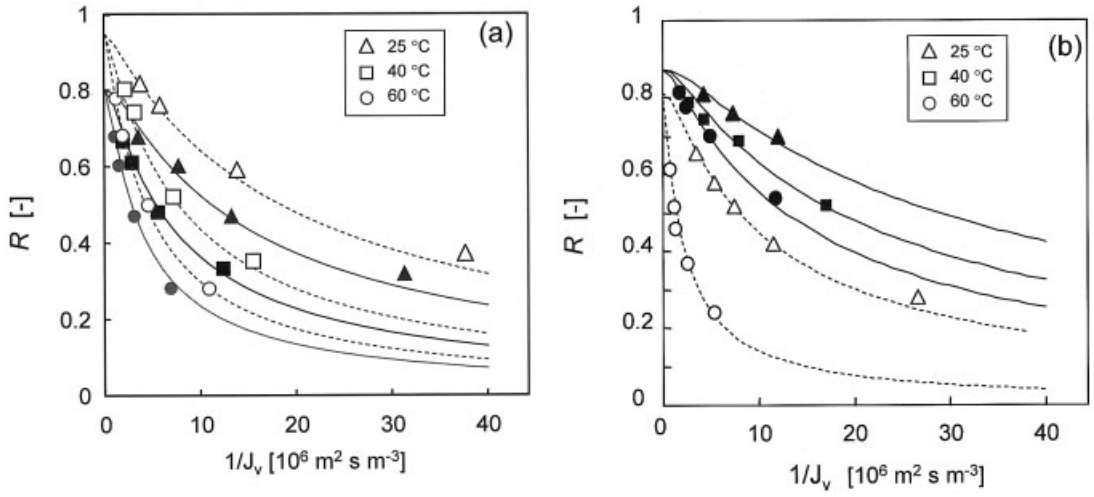

Figure 6. (a) (b) Rejection as a function of $1/J_v$ for decane (closed keys) and decanol (white symbols) (a), and for teradecane (black symbols) and octanol (white symbols) (b) in ethanol solutions (M-1.0): points are experimental, and curves are calculated with fitted σ and P.

shows similar data for octanol and teradecane. The dependency of rejection, R, on permeate flux, J_v, was curve-fitted to Eqs. 4-6 with a sufficient accuracy, as shown in Figures 6a and b, to permit membrane parameters, reflection coefficient σ, and solute permeability P to be obtained. It should be noted that concentration polarization always occurs as a result of the selective permeation of a solvent and a solute; however, in the present experimental conditions, no consideration of the boundary layer was required because the permeate volumetric flux, J_v, was in the range of 10^{-7}-10^{-6} m s^{-1}, which is sufficiently small to permit the effect of concentration polarization to be neglected, since the boundary-layer mass-transfer coefficient was estimated to be in the order of 10^{-5} m s^{-1} in a previous article.[21]

σ can be interpreted as rejection at an infinitely high flux, that is, graphically the intercepts at the ordinate of the fitted curves. Curve-Fitting was successfully carried out on the assumption of constant σ, irrespective of the permeation temperatures, which was found to be consistent with the case of aqueous systems using porous inorganic membranes.[21] This is probably because the reflection coefficient of porous membranes is dominantly determined by geometric conditions, that is, the ratio of the molecular seize of a solute to the pore size of a membrane, for the case of a molecular sieving mechanism. Consequently, the dependency of rejection can be attributed to that of solute permeabilities, which is the same conclusion drawn for aqueous solutions using polymeric membranes[24] and inorganic membranes.[21] Another membrane parameter is pure solvent permeabilities, L_p. As shown in Figure 4, the permeate flux, J_w, was approximately linear with the applied pressure, because the feed concentration of the solutes was sufficiently small to permit the osmotic pressure to be neglected. The osmotic pressure differences showing rejection of 0.5 were calculated as approximately 0.2 MPa on the assumption of an ideal solution. Volumetric solvent permeabilities, L_p, were obtained as the slopes of the permeate volumetric flux, J_v, against the transmembrane pressure, ΔP. Table 1 summarizes the membrane parameters, σ, P, and L_p, for alkanes and alcohols for M-1.0.

Temperature dependency of membrane parameters

The temperature dependency of solvent permeabilities is shown in Figure 7 as $L_p\mu_b$, that is, L_p multiplied by the viscosity in bulk solvents, μ_b. If the transport mechanism through nano-sized pores obeys the viscous flow mechanism with the same viscosity as in a bulk solution, $L_p\mu_b$ should be constant since structured parameters: r_p, N, and Δx in Eq. 3, are

Table 1. Reflection Coefficients, σ, Solute Permeability, P, and Pure Solvent Permeability, L_p, at Different Temperatures (M-1.0)

		$P \times 10^6$ [m · s^{-1}]			$L_p \times 10^{13}$ [m s^{-1} · Pa^{-1}]		
Solutes	σ [−]	25°C	40°C	60°C	25°C	40°C	60°C
hexane	0.74	0.28	0.52	1.12	0.97	1.93	3.85
decane	0.80	0.06	0.13	0.25	0.86	1.78	3.32
tetradecane	0.87	0.03	0.04	0.06	0.76	1.21	1.97
hexanol	0.78	0.40	—	1.60	1.12	—	3.96
octanol	0.81	0.09	—	0.50	0.95	—	3.90
decanol	0.95	0.05	0.12	0.22	0.83	1.57	3.24
pure EtOH*	—	—	—	—	1.06	1.87	4.11

*Viscosity of EtOH in bulk at 25, 40, and 60°C is 1.071, 0.803, and 0.577 mPa · s, respectively.

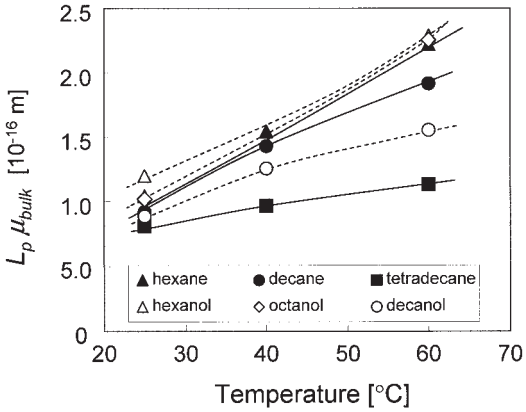

Figure 7. Temperature dependency of $L_p\mu_b$ for alcohols (white symbols) and alkanes (black symbols) in ethanol solutions.

(M-1.0; μ_b in mixtures was assumed to be the same as that of pure ethanol because of the low solute concentration).

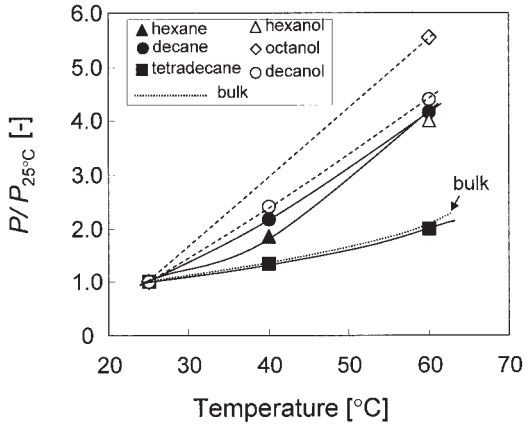

Figure 8. Temperature dependency of solute permeabilities, *P*, normalized at 25°C for alcohols (white symbols, broken curves) and alkanes (black symbols, solid curves) in ethanol solutions (M-1.0; temperature dependency of the diffusivity in bulk estimated by Wilke-Chang is shown with a dotted curve).

considered to be reasonably constant. As shown in Figure 7, $L_p\mu_b$ was not a constant and was found to increase with temperature. Therefore, it is obvious that the temperature dependency of solvent viscosities for pore sizes of 1 nm (M-1.0) is different from that in bulk solutions, that is, larger than that of a bulk solution. The observed activation energy of pure ethanol through M-1.0, obtained from an Arrhenius plot of L_p, was calculated to be 32 kJ·mol^{-1}. For the case of the viscous flow mechanism, the value is 14.6 kJ·mol^{-1}. This dependency has been reported for ceramic porous membranes with pore sizes in the nano-meter level[9,11,21] and can be interpreted as the interaction between permeating molecules and the membrane pore wall. Ternan[25] assumed the field forces (Van der Waals' forces) from a pore wall caused solvent in its vicinity to be more viscous than in bulk in order to explain the hindered diffusion in liquid-filled pores.[16] Based on diffusion experimental data using powdered adsorbents, he obtained a viscosity parameter, P_{vis}, the ratio of the enhanced viscosity to bulk viscosity, and showed that P_{vis} decreased with temperature. In the present study, in which porous membranes were used, the measurement of L_p, has a great advantage in the direct measurement of the temperature dependency of liquids in nano-sized pores.

Another explanation, based on the adsorption of permeating molecules, is also possible.[9,26] Ethanol, a polar molecule, can adsorb to a silica-zirconia pore wall that is covered with silanol groups (-SiOH). The adsorbed molecules might be immobilized or less mobile than the molecules in bulk, resulting in hydrodynamic resistance to the permeation of solvents. At higher temperatures, the amount adsorbed would decrease, resulting in a decreased viscosity. Another point that should be noted is the difference in solvent permeabilities among the types of solutes at a concentration of 1 mol %. Solvent permeabilities appear to decrease with an increase in solute size for alkanes as well as alcohols, although pure ethanol was permeated before each reverse osmosis experiment so as to recover approximately to the same level of permeate flux as the initial flux of ethanol. This is probably caused by pore-plugging by large linear molecules that were approximately the same size as the pore sizes.

Since solute permeability, *P,* is expressed by the effective diffusivity divided by membrane thickness, as shown in Eq. 5, *P* is considered to show the same temperature tendency as D_{eff}. Figure 8 shows the temperature dependency of *P* normalized with that at 25°C as a function of temperature, together with the case of bulk diffusivity, as estimated by the following Wilke-Chang equation, which is the most widely used equation for predicting viscosity:

$$D_{bulk} = 7.4 \times 10^{-12} \frac{(\phi M_B)^{1/2} T}{\mu_B V_A^{0.6}} \tag{12}$$

where ϕ is an association factor of solvent B (= 1.5 for ethanol), M_B is a molecular weight of solvent B in g·mol^{-1}, T is the absolute temperature in K, μ_B is the solvent viscosity in

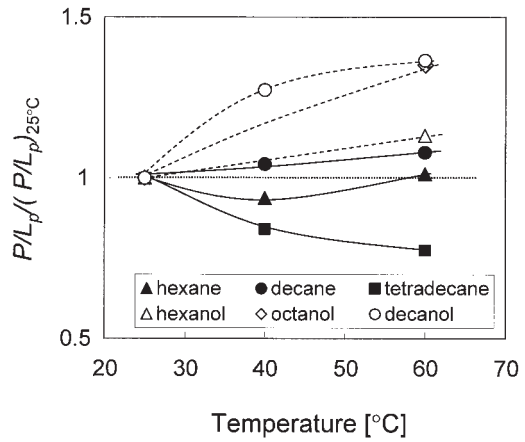

Figure 9. Temperature dependency of P/L_p of alcohols (white symbols , broken curves) and alkanes (black symbols, solid curves) in ethanol solutions (M-1.0; normalized at 25°C).

Table 2. Observed Activation Energy for Solution Permeability, L_p, Solute Permeability, P, and P/L_p. (M-1.0)

Solutes	ΔE [kJ · mol^{-1}]		
	L_p [m · s^{-1} · Pa^{-1}]	P [m · s^{-1}]	P/L_p [Pa]
decane	31.7	33.5	1.7
decanol	27.5	34.6	7.1
bulk*	14.6	17.2	2.6

*Activation energies of L_p and P in bulk solutions were calculated from the inverse of viscosity and Wilke-Chang equation from 25–60°C, respectively.

centipoises, and V_A is the molar volume of solute A in cm^3·mol^{-1} at its normal boiling temperature. As is clear from the Figure, the temperature dependency for solute diffusion through nano-sized pores, that is, hindered diffusion, is larger than the case of bulk diffusion. This tendency is in good agreement with the case of aqueous solutions obtained for inorganic membranes[21] as well as powdered adsorbents.[26,27]

Figure 9 shows values of P/L_p normalized with that at 25°C. According to the Wilke-Chang equation, diffusivity is expressed as the inverse of the solvent viscosity. Since L_p includes the viscosity of the permeating solutions in the denominator of Eq. 3, the effect of viscosity on permeability can be eliminated by plotting P/L_p as a function of temperature. Normalized P/L_p of alkane solutes are found to be approximately 1, which indicates that alkane permeabilities in membrane pores increase with temperature in the same manner as the inverse of solvent viscosities in membrane pores. This is also understandable based on transport equations. The permeate volumetric flux, J_v, can be considered to be the product of L_p and the applied pressure ΔP (Eq. 1) at dilute concentrations; therefore, J_v/P in Eq. 6 can be expressed as $(L_p/P)\Delta P$. If σ is constant, P/L_p needs to be approximately constant, irrespective of temperatures, so that rejection is dependent on transmembrane pressures and independent of permeation temperatures. This is why the rejection of alkanes was independent of temperature, as shown in Figures 4 and 5. On the other hand, P/L_p for alcohol solutes increased with temperature, indicating that the permeability increased with temperature more rapidly than the inverse of the viscosity in silica-zirconia pores. This explains why the rejection of alcohols decreased with temperature, as shown in Figures 4 and 5, and might be caused by a larger interaction with the pore wall for alcohol solutes than for alkane solutes.

Table 2 summarizes the observed activation energies for solvent permeability, L_p, solute permeability, P, and P/L_p for decane and decanol solutes, together with those in bulk solutions. The activation energies for solvent permeability, which reflects the temperature dependency of the viscosity inside the nano-sized pores, were approximately 30 kJ·mol^{-1}, larger than the case for the viscous flow mechanism. Solute permeabilities, which reflect the diffusivity, also show larger activation energies, in the range of 30-35 kJ·mol^{-1}, than in bulk (17.2 kJ·mol^{-1}). It should be noted that the activation energy of configuration diffusion has been reported to be in the range of 10-60 kJ mol^{-1} by Xiao and Wei.[28] The activation energies for diffusion in the liquid phase inside the nano-sized pores were found to be mainly contributed to by those for the viscosity. In terms of P/L_p, the activation energy of decane (1.7 kJ·mol^{-1}) was almost the same as that in bulk (2.6 kJ·mol^{-1}), while that of decanol (7.1 kJ·mol^{-1}) was larger than in bulk. This difference in activation energy of P/L_p explains the experimental findings showing that the rejection of alcohols decreased with temperature, while that of decane remained nearly constant. Thus, the effect of viscosity on diffusivity can be discussed separately by means of a data analysis of membrane separation in reverse osmosis, giving deep insights into transport parameters, such as viscosity and diffusivity, inside nano-sized pores.

Permeability determined by diffusion experiments and its comparison with that by reverse osmosis

Solute permeability, which is a quite important membrane parameter, can be determined based on two different experimental techniques: reverse osmosis experiments as described in the proceeding sections, and diffusion experiments. In Figures 10a and b, $\ln\{1 - (C_2/C^\infty)\}$, the left side of Eq. 10, is plotted as a function of time for the case of decane and hexane solutes,

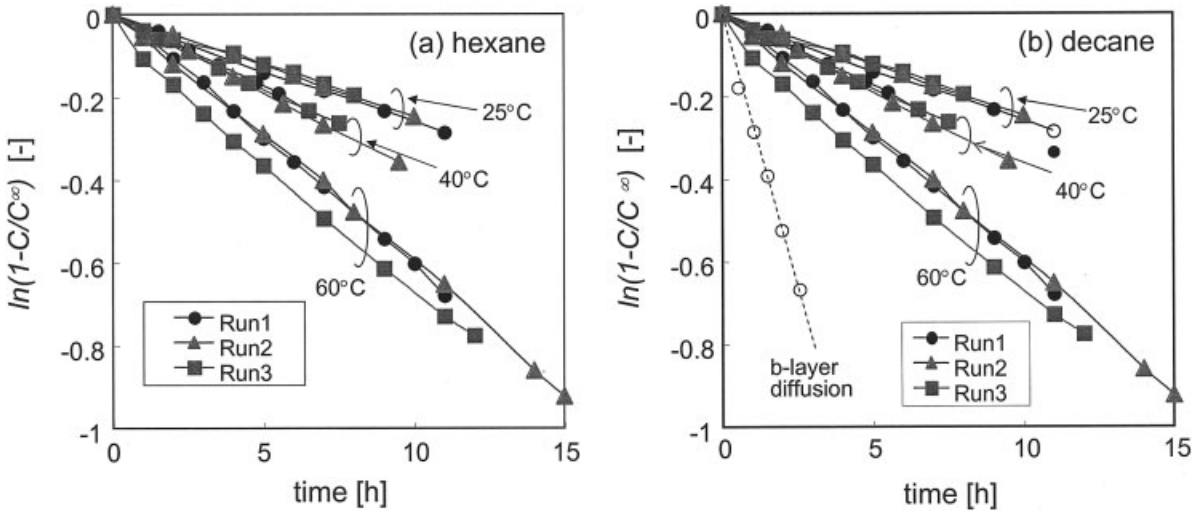

Figure 10. (a) (b) $\ln(1 - C_2/C^\infty)$ as a function of time at different temperature for hexane (a) and decane (b).

(M-1.0; $C_0 \cong C^\infty \cong 1$ mol %, $A = 27 \times 10^{-4}$ m^2; several runs were carried out at the same temperature. Diffusion data through b-layer (a supporting membrane without a separation layer) at 60° C is shown by an open circle in Figure 10b.)

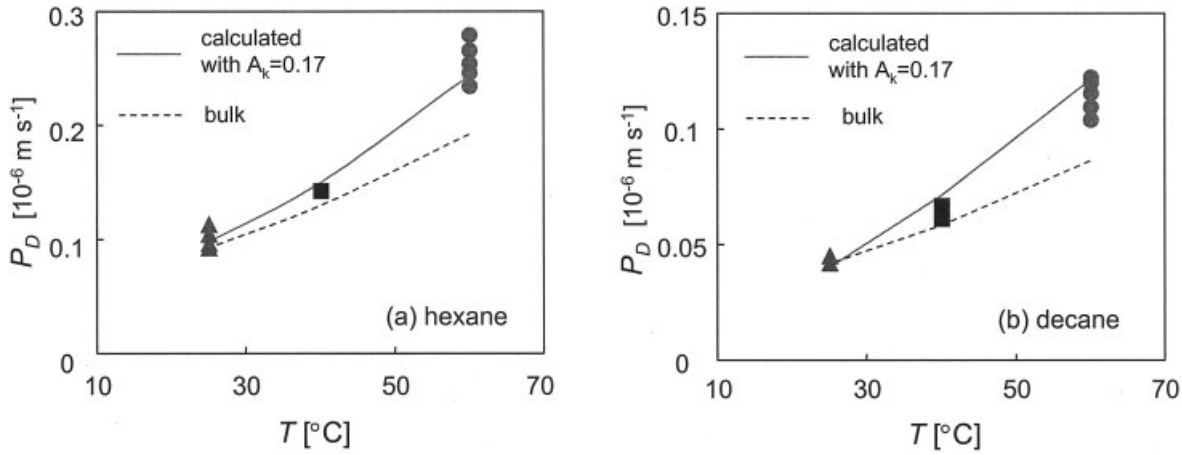

Figure 11. (a) (b) Solute permeabilities as a function of temperature for hexane (a) and decane (b).

(M-1.0; broken curves are predicted assuming bulk diffusivity; solid curves are predicted based on 2-layer model.)

respectively, at different temperatures. As shown in the Figures, the solute concentration increased more rapidly at high temperatures than at low temperatures in a quite reproducible manner. $\ln\{1 - (C_2/C^{\infty})\}$ decreased approximately linearly with time, and the slopes of the lines give the overall permeabilities, P_D, through a silica-zirconia membrane, M-1.0, which are plotted as a function of temperature in Figures 11a and b. The broken curves in the Figures indicate the predictions based on the overall permeability at 25° C and the temperature dependency of bulk diffusivity, indicating that P_D shows a larger temperature dependency than in bulk. The same conclusion, that the temperature dependency in nano-sized pores is different from that in bulk, as obtained from reverse osmosis experiments, was also drawn from diffusion experiments.

The membrane structures of most separation membranes, commercially available or laboratory-made, are asymmetric and mostly composite. As explained in the Experimental Procedures section, a top layer that has a separation ability is coated on a supporting membrane that has no separation ability; therefore, a bilayer model where the composite membranes consist of a separation layer (a-layer) on a support layer (b-layer) was postulated for the analysis of the diffusion experiments. According to the bilayer model, originally proposed by Kedem and Katchalsky[29] and experimentally verified by Johnson and Benavente,[30] the overall permeability P_D is given as the sum of the a- and b-layers, as follows:

$$1/P_D = 1/P_a + 1/P_b \tag{12}$$

Diffusion experiments show that the overall permeability, P_D, that is, the contribution of the a-layer and the b-layer, should be considered, since molecules diffuse across the membrane thickness along the concentration difference. On the other hand, reverse osmosis experiments show that P_a, that is, P in Eq. 5, is equal to P_a, since the solutes are separated in the a-layer and transported by convection through the b-layer, which has no separation ability.[30] P_a, determined by reverse osmosis experiments and summarized in Table 1, is found to be larger than P_D determined by diffusion experiments and shown in Figures 11a and b. The permeability of b-layer, P_b, with surface porosity, $A_{k,b}$, and the thickness of the b-layer, Δx_b, can be estimated similar to Eq. 5 as follows[19]:

$$P_b = D_{bulk}A_{k,b}/\Delta x_b = D_{bulk}\varepsilon_b/(\tau_b \Delta x_b) \tag{13}$$

Therefore, permeabilities, P_D, can be obtained as the sum of the b-layer permeability, P_b, calculated using Eq. 13 as a parameter of $A_{k,b}$, and the a-layer permeability, P_a, which is shown in Table 1. Good agreement was obtained at an $A_{k,b}$ of 0.17 between the experimental and calculated permeabilities, P_D, as shown in Figure 11a. The diffusion experiment of decane, as shown in Figure 11b, also confirms that a value of $A_{k,b}$ of 0.17 shows quite good agreement. It should be noted that A_k in Eq. 13 can be interpreted as the product of the porosity, ε_b, and the inverse of the tortuosity factor, τ_b. The membrane supports of the present study have an ε_b of 0.5; therefore, τ_b is estimated to be 2.9, which falls in a reasonable range of the tortuosity factors for porous materials reported in several literatures.[16] Moreover, the permeability of decane through the b-layer was obtained by a diffusion experiment through a supporting membrane without a separation layer, which had a thickness of 1 mm; the time course for the concentration change is shown in Figure 10b. Values of $A_{k,b}$ obtained by three different experiments are summarized in Table 3, and are in good agreement with each other. In conclusion, the diffusivity of solutes through nano-sized pores was confirmed to show a larger temperature dependency than in bulk, and also was in agreement with the dependency obtained by reverse osmosis experiments.

Table 3. Surface Porosity of the b-Layer, $A_{k,b}$, by Three Different Experiments

Membrane	M-1.0 (Separation Layer (a-layer) + Supporting Layer (b-layer))		Supporting Layer (b-layer)
Solutes	Hexane	Decane	Decane
$A_{k,b}$	0.17*	0.17*	0.18**

*$A_{k,b}$ was obtained by fitting experimentally obtained P_D with Eqs. 12 and 13.
**$A_{k,b}$ was obtained by diffusion experiment of a supporting membrane (b-layer) with Δx_b = 1 mm (the thickness of a supporting membrane).

Conclusions

Silica-Zirconia porous membranes with pore sizes from 0.8 to 2.5 nm were prepared by a sol-gel process, and used in the reverse osmosis of dilute solutions of alcohols and alkanes in ethanol.

Silica-Zirconia membranes with a 1 nm pore diameter showed a MWCO of 200, and were found to be applicable to the separation of mixtures of organic solvents.

Reverse osmosis experiments confirmed that the viscosities of solutions in nano-sized pores showed a larger temperature dependency than in bulk. The diffusivities of alkane and alcohol solutes were found to show larger temperature dependency than in bulk based on reverse osmosis experiments as well as diffusion experiments.

The diffusivity of alkanes shows the same temperature dependency as the viscosity of ethanol in nano-sized pores, since P/L_p for alkanes was approximately constant. On the other hand, the diffusivity of alcohols shows a larger temperature dependency than that for the viscosity of ethanol, probably because of larger interaction between the solute and the hydrophilic surface of silica-zirconia membranes.

A bilayer model verified that solute permeabilities by reverse osmosis and diffusion are consistent with each other.

Notation

A_k = surface porosity
C = concentration, $mol \cdot m^{-3}$
D = diffusivity, $m^2 \cdot s^{-1}$
J_w = weight-based flux, $kg \cdot m^{-2} \cdot s^{-1}$
J_v = volume-based flux, $m^3 \cdot m^{-2} \cdot s^{-1}$
L_p = solvent permeability, $m^3 \cdot m^{-2} \cdot s^{-1} \cdot Pa^{-1}$
N = number of pores, m^{-2}
P = permeability, $m \cdot s^{-1}$
R = rejection of solutes
σ = reflection coefficient
r_p = pore radius, m
V = volume of diffusion cell, m^3
Δx = membrane thickness, m
μ = viscosity, Pa·s
ϕ = association factor

Subscripts

f, p = feed stream, permeate stream
b = bulk
1, 2 = feed and permeate stream in diffusion experiments, respectively

Superscripts

0 = initial
∞ = final

Literature Cited

1. Machado DR, Hasson D, Semiat R. Effect of solvent properties on permeate flow through nanofiltration membranes. *Journal Membrane Science.* 2000;166:63-69.
2. Whu JA, Baltzis BC, Sirkar KK. Nanofiltration studies of larger organic microsolutes in methanol solutions. *Journal Membrane Science.* 2000;170:159-172.
3. Bhanushali D, Kloos S, Bhattacharyya D. Solute transport in solvent-resistant membranes for non-aqueous systems: experimental results and the role of solute-solvent coupling. *Journal Membrane Science.* 2001;208:343-359.
4. Peeva LG, Gibbins E,. Luthra SS, White LS, Stateva RP, Livingston AG. Effect of concentration polarization and osmotic pressure on flux in organic solvent nanofiltration. *Journal Membrane Science.* 2004; 236:121-136.
5. Geens J, Bruggen BV. Vandecasteele C. Characterization of the solvent stability of polymeric nanofiltration membranes by measurement of contact angles and swelling. *Chemical Engineering Science.* 2004; 59:1161–1164.
6. Gestel TV, Bruggen BV, Buekenhoudt A, Dotremont C, Luyten J, Vandecasteele C, Maes G. Surface modification of Al_2O_3/TiO_2 multilayer membranes for applications in non-polar organic solvents. *Journal Membrane Science.* 2003;224:3-10.
7. Guizard C, Ayral A, Julbe A. Potentiality of organic solvents filtration with ceramic membranes. A comparison with polymer membranes. *Desalination.* 2002;147:275-280.
8. Tsuru T. Inorganic porous membranes for liquid phase separation. *Separation and Purification Methods.* 2001;30:191-220.
9. Tsuru T, Sudoh T, Kawahara S, Yoshioka S, Asaeda M. Permeation of liquids through inorganic nanofiltration membranes. *Journal of Colloid and Interface Science.* 2000;228:292-296.
10. Buekenhoudt A, Dotremont C, Aerts S, Vankelecom I, Jacobs P. Successful application of ceramic nanofiltration in non-aqueous solvents. Proceedings of Eighth International Conference on Inorganic Membranes, Cincinnati, USA, 2004: 278-281.
11. Tsuru T, Kondo H, Yoshioka T, Asaeda M. Permeation of nonaqueous solution through organic/inorganic hybrid nanoporous membranes. *AIChE Journal.* 2004;50:1080-1087.
12. Tsuru T, Sudoh T, Yoshioka T, Asaeda M, Nanofiltration in non-aqueous solutions by inorganic porous membranes. *Journal Membrane Science.* 2001;185:253-261.
13. Tsuru T, Miyawaki M, Kondo H, Yoshioka T, Asaeda M. Inorganic porous membranes for nanofiltration of nonaqueous solutions. *Separation Purification Technology.* 2003;32:105-109.
14. Mulder, M. *Basic Principles of Membrane Technology*. *Dordrecht:* Kluwer Academic Publishers; 1996.
15. Spiegler KS, Kedem O. Thermodynamics of hyperfiltration (reverse osmosis) criteria for efficient membranes. *Desalination.* 1996;1:311-326.
16. Kärger J, Ruthven DM. *Diffusion in Zeolites and Other Microporous Solids*. New York: Wiley, 1992.
17. Chantong A, Massoth FE. Restrictive diffusion in aluminas. *AIChE Journal.* 1983;29:725-731.
18. Poling BE, Prausnitz JM, O'Connell JP. *The Properties of Gases and Liquids*. New York: McGraw-Hill, 2000.
19. Nakao S. Membrane transport phenomena and ultrafiltration. In: *Encyclopedia of Fluid Mechanics*. Cheremisinoff NP (ed.). Houston: Gulf Publishing Company; 1986:987-1028.
20. Deen WM. Hindered transport of large molecules in liquid-filled pores. *AIChE Journal.* 1987;33:1409-1425.
21. Tsuru T, Izumi S, Yoshioka T, Asaeda M. Effect of temperature on transport performance of neutral solutes through inorganic nanofiltration membranes. *AIChE Journal.* 2000;46:565-574.
22. Tsuru T, Wada S, Izumi S, Asaeda M. Preparation of microporous silica-zirconia membranes for nanofiltration. *Journal Membrane Science*. 1998;149,127-135.
23. Tsuru T, Hino T, Yoshioka T, Asaeda M. Permporometry characterization of microporous ceramic membranes. *Journal Membrane Science.* 2001;186:257-265.
24. Nomura T, Nakao S. Kimura S. Influence of feed temperature on ultrafiltration performance. *Kagaku Kogaku Ronbunshu.* 1987;13:811-817.
25. Font J, Castro RP, Cohen Y. On the loss of hydraulic permeability in ceramic membranes. *Journal of Colloid and Interface Science.* 1996; 181:347-350.
26. Ternan M. The diffusion of liquid in pores. *Canadian Journal of Chemical Engineering.* 1987;60:244-249.
27. Seo G, Massoth FE. *AIChE Journal.* 1985;31:494-496.
28. Xiao J, Wei J. Diffusion mechanism of hydrocarbon in zeolites—1. *Theory Chemical Engineering Science.* 1992;47:1123-1141.
29. Kedem O, Katchalsky A. Permeability of composite membranes. *Transactions of the Faraday Society.* 1963;59:1941-1953.
30. Johnson G, Benavente J. Determination of some transport coefficients for the skin and porous layer of a composite membrane. *Journal Membrane Science.* 1992;69:29-42.

Manuscript received May 9, 2005, and revision received Jun. 30, 2005.